



HAL
open science

Bi-Layer textures: a Model for Synthesis and Deformation of Composite Textures

Geoffrey Guingo, Basile Sauvage, Jean-Michel Dischler, Marie-Paule Cani

► **To cite this version:**

Geoffrey Guingo, Basile Sauvage, Jean-Michel Dischler, Marie-Paule Cani. Bi-Layer textures: a Model for Synthesis and Deformation of Composite Textures. Computer Graphics Forum, 2017, Proceedings of EGSR, 36 (4), pp.111-122. 10.1111/cgf.13229 . hal-01528537

HAL Id: hal-01528537

<https://hal.science/hal-01528537>

Submitted on 31 May 2017

HAL is a multi-disciplinary open access archive for the deposit and dissemination of scientific research documents, whether they are published or not. The documents may come from teaching and research institutions in France or abroad, or from public or private research centers.

L'archive ouverte pluridisciplinaire **HAL**, est destinée au dépôt et à la diffusion de documents scientifiques de niveau recherche, publiés ou non, émanant des établissements d'enseignement et de recherche français ou étrangers, des laboratoires publics ou privés.

Bi-Layer textures: a Model for Synthesis and Deformation of Composite Textures

Geoffrey Guingo^{1,2}, Basile Sauvage², Jean-Michel Dischler² and Marie-Paule Cani¹

¹Université Grenoble Alpes, CNRS (LJK), and Inria, Grenoble, France

²ICube, Université de Strasbourg, CNRS, France

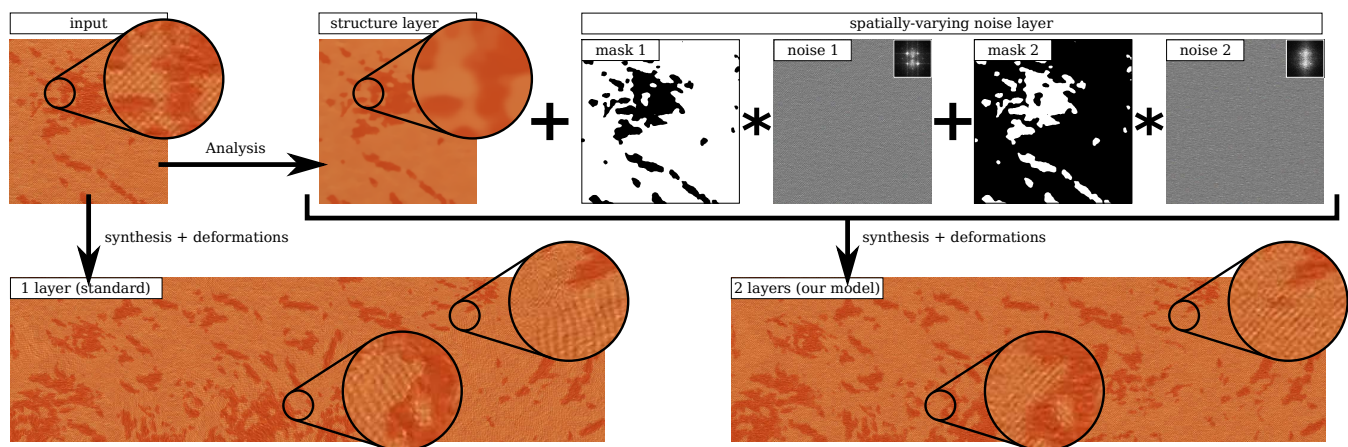


Figure 1: Our noise model decomposes an input exemplar as a structure layer and a noise layer. The noise layer captures a spatially varying Gaussian noise as a blend of stationary noises. Large outputs are synthesized on-the-fly by synchronized synthesis of the layers. Variety can be achieved at the synthesis stage by deforming the structure layer while preserving fine scale appearance, encoded in the noise layer.

Abstract

We propose a bi-layer representation for textures which is suitable for on-the-fly synthesis of unbounded textures from an input exemplar. The goal is to improve the variety of outputs while preserving plausible small-scale details. The insight is that many natural textures can be decomposed into a series of fine scale Gaussian patterns which have to be faithfully reproduced, and some non-homogeneous, larger scale structure which can be deformed to add variety. Our key contribution is a novel, bi-layer representation for such textures. It includes a model for spatially-varying Gaussian noise, together with a mechanism enabling synchronization with a structure layer. We propose an automatic method to instantiate our bi-layer model from an input exemplar. At the synthesis stage, the two layers are generated independently, synchronized and added, preserving the consistency of details even when the structure layer has been deformed to increase variety. We show on a variety of complex, real textures, that our method reduces repetition artifacts while preserving a coherent appearance.

CCS Concepts

•Computing methodologies → Texturing;

1. Introduction

Textures efficiently enhance objects with fine colored details and have therefore been ubiquitous for a long time in 3D virtual scenes. The recent improvements of graphics hardware and rendering techniques support the demand for increasingly detailed visual content.

In this context, by example texture synthesis, which allows the automatic generation of textures from small size exemplars, has become a major challenge. It can either be used to support otherwise painstaking manual texture creation (enabling artists to focus manual edits where needed the most), or as an alternative to it.

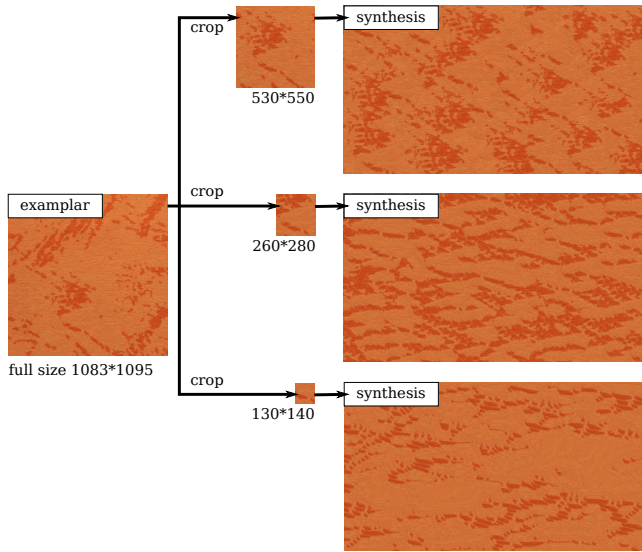


Figure 2: What you see is all you get: the smallest the input the more repetitive the output, even using off-line optimization techniques [KNL*15].

By example texture synthesis makes the fundamental assumption that the exemplar is representative of the underlying natural texture. Unfortunately, this assumption turns out to be wrong in many cases: exemplars are generally too small to cover the entire visual span of a given texture, leading to visual artifacts. As shown in Figure 2, even the best optimization techniques cannot provide more variety than the exemplar. This strongly hampers realism. Moreover, optimization leads to heavy computations and produces textures that are bounded.

Gaussian noise and tile-based methods are two alternative approaches for generating unbounded textures on-the-fly (i.e. at runtime), from a single input exemplar. Whereas noise by example inherently avoids repetition artifacts, it can only handle homogeneous textures and hardly manages non-Gaussian patterns, which represent the very large majority of textures. In reverse, tile-based methods, such as Wang tiles, are able to reproduce complex, non-Gaussian patterns with spatial variations, but since tiles are pre-generated using traditional synthesis approaches (like Graph-cut or optimization), they typically exhibit the previously mentioned strong repetition artifacts. The intuition is that spatial deformations can help to significantly reduce repetitions. However, if not done properly, fine scale patterns may be ruined, as shown in Figure 1 bottom-left and Figure 3 top. Several works apply deformations in the synthesis process to create more varied contents, but the proper use of deformation has not been deeply tackled so far.

Our goal is to propose a more general, infinite on-the-fly texture synthesis method, able to introduce variety when synthesizing natural textures. Many natural textures are composite, i.e. they exhibit different patterns at different locations (see dark and light patterns in Figure 1). The variety lies in the structure (i.e. the shape, size and orientation of large patterns) while the consistency lies in the homogeneity of fine scale patterns. To achieve this, the insight

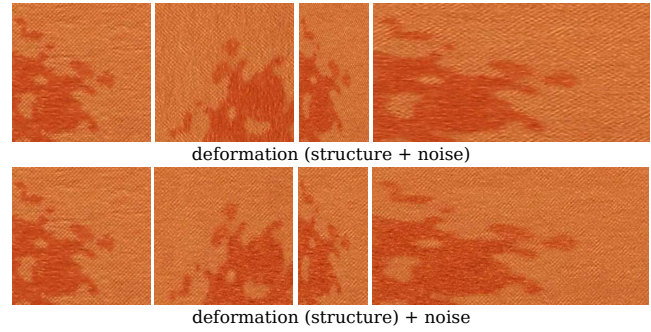


Figure 3: Pattern deformations produce variety provided that fine grain appearance is preserved: rotation and stretching are shown on the usual 1-layer textures (top) versus our 2-layer model (bottom). Our model enables to deform structured patterns while preserving fine scale noisy patterns.

is to exploit the complementary nature of noise-based versus tile-based methods. The texture is decomposed into two additive layers: a structure layer captures spatial variations and non-Gaussian patterns, and is synthesized using tile-based approaches augmented by deformations (scaling, rotations and stochastic distortion fields); a noise layer captures fine scale Gaussian patterns and is synthesized with procedural methods. This solution implies solving two core issues: on the analysis side, quantifying noise and separating it from structure, as illustrated in Figure 1 top; and on the synthesis side, making the noise vary spatially according to the synthesized structure. A major advantage of this bi-layered model is that deformations of the structure produce variety while fine-scale consistency is maintained, as shown in Figure 3 bottom.

Our model is encoded using a combination of images (defining the structure), power spectrum densities (defining noises), and masks (synchronizing noises over the structure). The main contributions are:

- A new model for spatially varying Gaussian noise: a few stationary noises are blended according to masks that encode non-stationarity (Section 3). To the best of our knowledge, this is the first method to analyze, describe and synthesize Gaussian noise with spatial variations. The key difficulty that we solve here is the spectrum estimation in the presence of spatial variations. We use clustering in the spectral domain and a new technique for computing power spectrum densities (PSD) through auto-correlation while some data is missing.
- A new bi-layered texture model: a noise layer captures fine scale Gaussian patterns, while a structure layer captures non-Gaussian patterns and structures (Section 4). The key idea is to synchronize the layers through a set of masks enabling preservation of consistency. We can achieve unprecedented synthesis and deformation results compared to single layer models.
- An analysis method to instantiate our bi-layered model from a single input exemplar and very light user input (section 5). The two layers, the masks and the spectra of the Gaussian patterns are then automatically computed.

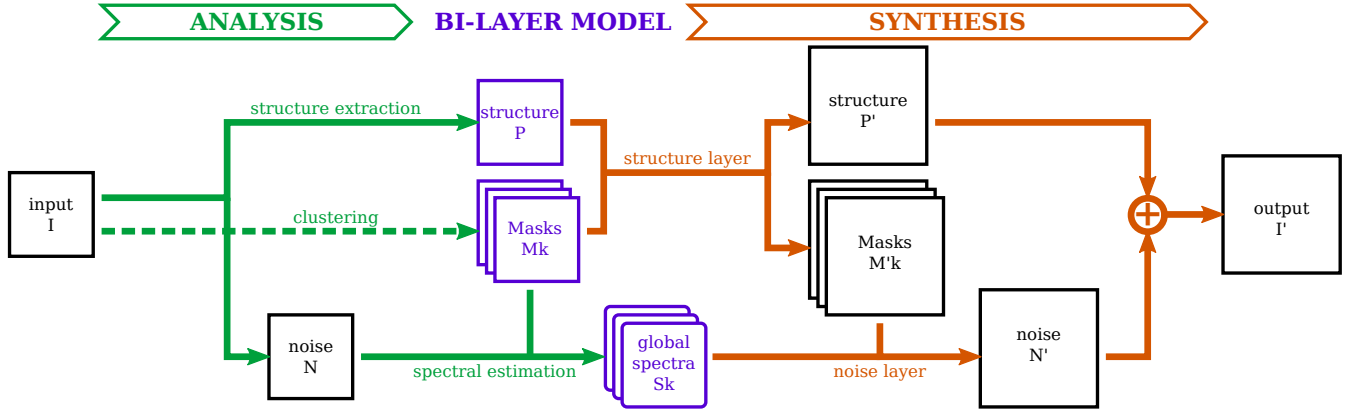


Figure 4: Processing pipeline. Our bi-layer model encodes textures using a structure layer (an image P), a set of Gaussian noises (spectra S_k) and a set of localization masks (M_k). Analysis (left) consists in instantiating the model from a single input exemplar I : the structure is extracted using filtering ($I = P + N$); the masks are computed using clustering; the spectra S_k are computed using a new technique based on auto-correlation. Synthesis (right) computes large composite outputs on-the-fly: a structure layer with masks is synthesized using a tile-based approach; a spatially-varying noise layer is synthesized procedurally from the spectra and the masks; the two layers are added to create the final texture.

For clarity reasons, these contributions are explained in separate sections 3 to 5. They enable by-example texture synthesis, as summarized by the pipeline depicted in Figure 4. An input exemplar I is analyzed (in green Figure 4):

- A structure layer P is extracted by filtering I (Section 5).
- A noise layer is computed as $N = I - P$.
- Masks M_k are computed using clustering in the spectral domain (Section 3.3). Each mask corresponds to one stationary noise.
- Global spectra S_k (one per noise) are computed (Section 3.3).

Then, from the bi-layer model –encoded by P , M_k and S_k –, an output texture $I' = P' + N'$ is synthesized as the sum of two layers (in orange Figure 4):

- The structure layer P' is synthesized using tile-based methods. Masks M'_k are synthesized at the same time so as to encode synchronization with the noise (Section 4).
- The spatially-varying noise layer N' blends stationary noises (according to M'_k , see Section 3.2) which are computed from their spectra S_k by any state-of-the-art algorithm.

2. Related work

Most texture synthesis works address off-line synthesis [WLKT09], using for instance global optimization methods as initiated by [KEBK05]. But there is a recent need for "on-demand" generation of arbitrary sub-parts of a texture, as necessary for unbounded on-the-fly texturing. Our work belongs to these on-the-fly texture synthesis methods. It is also related to texture synthesis with spatial deformation and to noise by example.

2.1. On-the-fly texture synthesis

By example on-the-fly texture synthesis methods can be classified into two approaches: 1) parallel, data-driven algorithms, 2) tiling techniques. On-the-fly data driven algorithms implement parallel

variants of pixel and patch-based synthesis algorithms, and suffer from the same limitations as their non-parallel counterparts. While parallel pixel-based approaches [LH05] require a feature map to preserve structure, parallel patch-based techniques [LL12] may produce visual repetition as well as possible seams. In both cases, the computational load is high, since these methods operate on full neighborhoods, as opposed to individual surface points. These neighborhoods must be stored in a cache and are frequently accessed within iterative procedures, which reduces performance.

Tile-based techniques consist in creating puzzles, but (in contrast with patch-based methods) use a pre-computed set of well-connecting texture tiles to generate an aperiodic tessellation of the plane. They are much faster than the previous parallel approaches and are thus better suited for real-time rendering applications. The pieces can either be generated from an exemplar, such as Wang and corner tiles [CSHD03, LD06] or computed procedurally [Sta97]. Patches with irregular shape have been used in [VSLD13], using an additional indirection to get rid of the explicit storage of large numbers of pre-computed tiles. The core issue with these approaches is the fact that the same few pieces are repeated over and over again, since only the arrangements are random.

2.2. Texture synthesis with spatial deformation

By example synthesis methods never generate new texture features, so the result lacks visual variation if the supplied exemplar is too small or contains a salient and unique feature. A standard way of reducing feature repetition consists in applying noise-based spatial distortions (i.e. a random shift of texture coordinates), as done for near-regular textures in [LLH04] and for tile-based synthesis in [CJMW13]. This principle was introduced by Perlin [LLC*10] to add natural randomness to perfectly periodic structures. It was also experimented in [DG95], which argued that distortions should at least preserve some spectral characteristics of patterns such as

anisotropy. Some by example synthesis techniques have used deformation like the feature matching and deformation synthesis approach of [WY04] and the graph-cut texture synthesis [KSE*03]. In the latter case, deformation is used to give a perspective distortion impression. In all cases, the principle is simple: the deformation is applied to the input and added to the pool of potential patches / neighbors to select contents. But all techniques have a strong drawback: spatial distortions may corrupt the visual characteristics of "sub-patterns", as for instance a cement pattern on a brick that would be stretched at the same time as the brick.

Our approach builds on tile-based methods. By separating noise patterns from structure, it improves the visual variety and extends the range of acceptable deformations: the structure can be distorted, stretched or rotated while the underlying noise patterns are preserved (see Figure 3).

2.3. Composite texture models

A composite texture model represents a texture as an assembly of simpler sub-textures. It is often defined as a two-layered model, where one layer is a label map indicating where the different sub-textures are located [ZFCVG05]. The label map defines a partition of the plane. Some methods first synthesize a label map, and then fill the result with different sub-textures [RCOL09]. There are however two difficult issues: segmenting an input image into sub-textures and synthesizing sub-textures by taking into account transitions between them. Optimization and off-line synthesis techniques can partly resolve the latter issue [WWY14].

At first glance, our approach resembles composite texture synthesis. However, it differs on a fundamental aspect: we do not use any label map, but only use additive layers. What we call "structure" in our model is a filtered color pattern image, as opposed to a label map. The filtered image is linearly combined with a weighted sum of stationary noises. This comes up with several advantages. Firstly, extracting "noise" is easier than texture segmentation, because a spectral metric can be used instead of texture classification algorithms [LSA*16]. Secondly, our structure can be synthesized with any existing on-the-fly tile-based synthesis technique [CSHD03, LD06, VSLD13], provided that we integrate into the procedure the weights of the different noises. Lastly, stationary noise can be easily synthesized on-the-fly using pseudo-random number generation.

2.4. Noise by example

Noise by example [GLLD12, GDG12] allows the generation of a parametric noise function from an example image. Such noises correspond to sub-classes of irregular textures, called Gaussian textures. Procedural noise inherently allows for infinite texturing without repetition. However, Gaussian textures are rare (actually, none of the textures found for instance in the textures.com database is Gaussian). The lack of structure can be addressed by fixing some phases in the power spectrum [GSV*14]. This approach is however biased since structure might be spread all over the spectrum, so a binary separation of frequencies is most often not adequate.

An efficient noise synthesis technique inspired by Spot-noise [vW91] has recently been proposed in [GLM17], based on

sparse convolution with a so-called "texton". The authors propose to mix noises by interpolating between textons, which allows for smooth spatial variations. However, no exemplar analysis is provided to separate different noises, and the method is restricted to Gaussian textures.

The random phase component is assumed stationary with all of these techniques. However, noise characteristics are not stationary for most natural textures. A similar problem appeared in [JCW11], where diffusion curves are textured using Gabor noise with spatially varying parameters, so as to get a vector representation of bitmap images. Gabor filter banks are applied on disks of 40 pixels diameter around the pixels to evaluate local main frequency components. But as mentioned by the authors, "this allows recording a single dominant frequency that captures only a rough impression of many textures". This is sufficient for image vectorization but not for texture synthesis. We show that large spectra are necessary to capture good quality noise patterns. One of our major contributions is to be able to evaluate such spectra using a novel approach based on auto-correlation.

The next section describes our new noise model. Its combination with a structure layer will be discussed in Section 4.

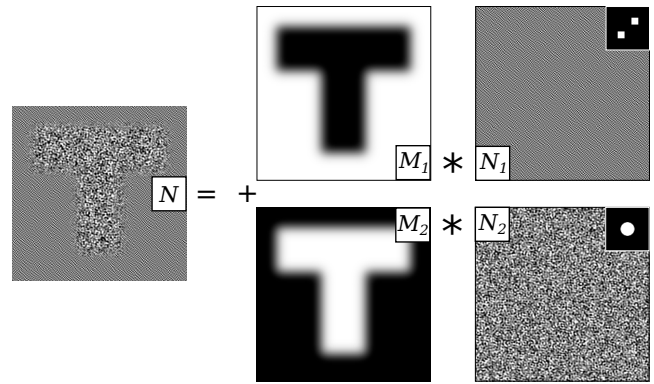


Figure 5: Spatially varying Gaussian noise. Each SV-noise (N) is a blend of stationary noises (N_k) defined by spectra (inset) and weighed by masks (M_k).

3. Spatially varying Gaussian noise

3.1. Stationary noise

A Gaussian noise is characterized by its power spectrum distribution (PSD), which represents how the power S^2 is distributed across frequencies f , where S is the magnitude of noise's spectrum (we will call S "spectrum" in the derivations below for readability).

Phase randomization, that we call Random-Phase Noise (RPN), is a technique to estimate a random realization of a stationary Gaussian noise from a given PSD:

$$RPN(x) = \sum_f S(f) \cos(fx + \varphi(f)) \quad (1)$$

where the phases $\varphi(f)$ are randomly picked. State-of-the-art models and algorithms are able to analyze a discrete input by computing its PSD and to synthesize on-the-fly a continuous non-repetitive

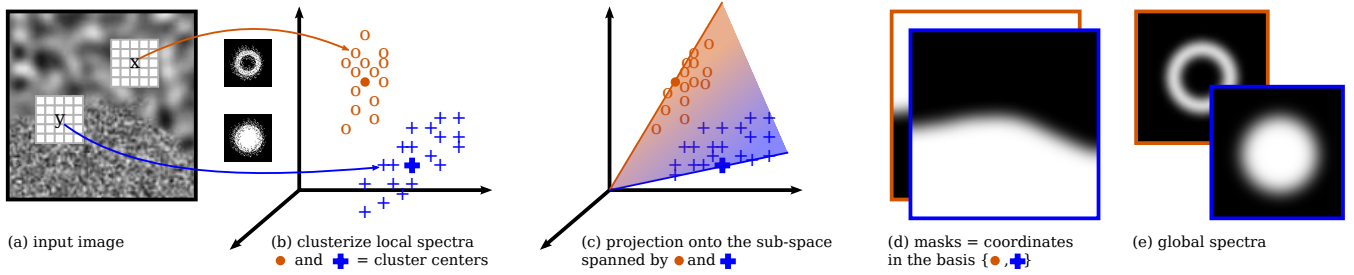


Figure 6: Noise by example: computation of masks and basis. Local spectra S_x^{loc} are computed by Welch’s method on small windows around pixels x of the input (a). A clustering (b) provides cluster centers S_k^{loc} which span a subspace onto which the local spectra are projected (c). The coordinates are forced to be positive to get the masks (d). The global spectra S_k are computed by our new estimator based on auto-correlation (e).

infinite output [GLLD12, GSV*14]. They rely on variants of Equation (1) so they assume stationarity, i.e. the spectrum S is assumed to be independent from the position x .

3.2. Spatial variations

To make the noise vary spatially, we would like the spectrum S to depend on the position x . We achieve this by defining a spatially-varying(SV)-noise N as:

$$N(x) = \sum_{k=1}^K M_k(x)N_k(x), \quad (2)$$

where M_k are scalar blending masks, and N_k are stationary noises described by “global” spectra S_k (see Figure 5). An advantage of this solution is to separate spatial variations – encoded in $M_k(x)$ – and spectral information – encoded $S_k(f)$.

The intuition is that, thanks to linearity of Equation (1), N is then characterized around x by the “local” spectrum $S_x(f) = \sum_k M_k(x)S_k(f)$, provided that the phases ϕ are the same for all k , that is the noise realizations are not independent. Enforcing ϕ this way solves for the optimal transport on the Gaussian distributions, which has been proven to be appropriate to interpolate Gaussian noises [XFPA14].

Based on state-of-the-art methods for stationary noises, SV-noise can be synthesized efficiently: each N_k is synthesized using a random phase approach (e.g. Equation (1) with $S = S_k$) or a sparse convolution [GLM17]; then they are blended with weights M_k . On-the-fly synthesis also requires the masks to be synthesized on-the-fly. This can be done using any state-of-the-art method, e.g. noise or tiles. We refer to Section 4 since synthesizing an SV-noise is a particular case of our two-layers model, where the structure layer is empty. Figure 5 shows a synthetic example of spatially-varying noise (SV-noise).

3.3. Noise by example

Let us now address the problem of instantiating the noise model of Equation (2) from an input exemplar: given a spatially varying noise exemplar I , we derive a set of masks $\{M_k\}$ and spectra $\{S_k\}$ in the following way. We view our model as a decomposition of

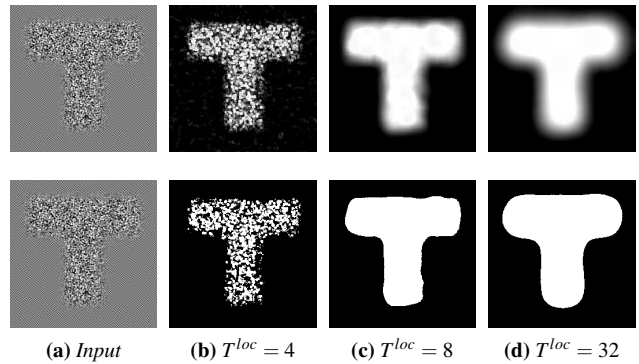


Figure 7: Computation of masks M_k from an SV-noise input (a). Top row: normalized distances $\|S_x^{loc} - S_k^{loc}\|$. Bottom row: binary masks. The larger T^{loc} the better the discrimination but the less precise the boundaries. A good strategy is to set T^{loc} as small as possible to get precise masks while still discriminating regions.

the noise in a basis $\{S_k\}$, where the masks $\{M_k\}$ used as weighing factors play the role of spatially-varying coordinates with respect to these noises. The difficulty is that neither the basis nor the coordinates are known. We solve the problem using the process illustrated in Figure 6, described next.

Mask estimation. First, we estimate the local spectra S_x^{loc} of size T^{loc} using Welch’s method [Wel67] in a small window centered at each pixel x . They describe the local frequency content around x . Then, we run a clustering algorithm on $\{S_x^{loc}\}$ to get K representative cluster centers S_k^{loc} , $1 \leq k \leq K$. We use a K-means algorithm with a number K of seeds provided by the user. Then, for each pixel, S_x^{loc} is projected onto the subspace spanned by the basis $\{S_k^{loc}\}$. The coordinates in this basis are the mask values $M_k(x)$, provided that they are positive.

We experimented several alternatives for projecting S_x^{loc} . Orthogonal projection is not appropriate because it provides many large or negative coordinates. So, we computed a convex barycenter of $\{S_k^{loc}\}$ that preserves the relative distances $\|S_x^{loc} - S_k^{loc}\|$. This is robust but boundaries are blurred, as shown in Figure 7: the larger T^{loc} the more robust, but the more blur. So T^{loc} must be

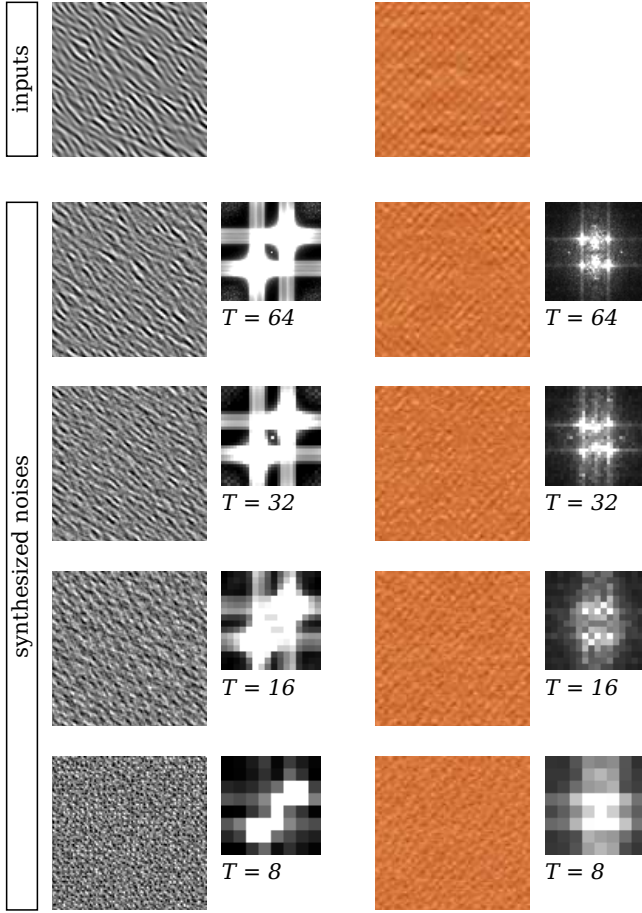


Figure 8: Noise synthesis. The larger the spectrum size T the better the reproduction. In all our examples we used $T = 64$.

large enough to capture the noise spectrum, although many natural textures exhibit sharp boundaries. Hence, when transitions are sharp we used binary masks. $M_k(x) = 1$ iff S_x^{loc} belongs to cluster k .

We could expect S_k^{loc} to be good estimates for S_k . However, estimating local spectra requires to use windows smaller than spatial variations, typically $4 \leq T^{loc} \leq 16$ for our examples, as illustrated in Figure 7. Conversely, spectra for synthesis must have much higher resolution, typically $T \geq 64$, as illustrated in Figure 8. Common spectrum estimation techniques require large windows of stationary signal. However, they cannot be applied in our case because of the spatial variations. So, we developed a new technique based on auto-correlation.

Spectral estimation with missing data. The PSD of a signal is equal to the Fourier transform of its auto-correlation AC . If I is a stationary signal with finite power, AC can be estimated over a $T \times T$ window Y by

$$AC_Y(x) = \frac{1}{|Y|} \sum_{y \in Y} I(y)I(y+x) \quad (3)$$

where positions $y+x$ are computed modulo T . In our case I is not stationary over large windows, but approximately piecewise stationary over regions within Y . We propose to estimate AC over the pairs of pixels lying both inside the region of interest:

$$AC_Y^M(x) = \frac{1}{|M \cap Y|} \sum_{y \text{ and } x+y \in M \cap Y} I(y)I(y+x) \quad (4)$$

where M is a binary mask of the region. The FFT of AC_Y^M provides a noisy estimate of the spectral content within the region. To reduce noise while maintaining the resolution, we make use of averaging. That is, we pave I with square windows Y and estimate the PSD as an average over the different windows, weighted by the number of pixels:

$$S^2 = \frac{1}{\sum |M \cap Y|} \sum |M \cap Y| \widehat{AC_Y^M}(f) \quad (5)$$

The estimator (5) is amazingly robust to regions with complex shapes and sparsity $|M \cap Y|/|Y| \geq 70\%$. We use it to estimate each S_k with M covering 90% of the cluster k (the 90% closest to S_k^{loc}). In practice we used $T = 64$ in all our examples.

Parameter tuning. We are left with two parameters. The first one is the number K of clusters, which is easy to provide: it equals the number of different random patterns perceptually salient to the user in the input exemplar, generally 2 to 4. The second parameter is the size T^{loc} of the local spectra. We refer the reader to Section 4 for a user-friendly technique to set it, based on visual evaluations.

4. Bi-layer textures

For clarity reasons, we present our model for greyscale textures and refer to section 6 for the management of colors. Our texture model is inspired by real textures, which often exhibit strongly structured patterns locally enhanced with noisy patterns. As shown in Figure 1 top, we decompose a texture I as a sum

$$I(x) = P(x) + N(x) = P(x) + \sum_{k=1}^K M_k(x)N_k(x), \quad (6)$$

where P is a structure layer and N is a spatially varying noise layer defined as in Section 3. Thus a texture is encoded by:

- P : an image representing the structure layer,
- S_k : scalar maps representing the spectra of noises N_k ,
- M_k : scalar maps representing the masks of noises N_k .

The motivation is to take benefits from the different synthesis techniques that can be used for the two layers (see Figure 4). To create a new texture image, a new structure layer P' together with new masks M'_k are first synthesized from P and $\{M_k\}$. State-of-the-art tile-based methods can be used at this stage because they are appropriate for highly structured textures. The masks are treated as extra channels that correlate with P : they undergo the same operations (cut, copy, paste, blend, deform) as P . In a second stage, an SV-noise layer is synthesized using the procedural methods described in Section 3. The key idea here is that the masks serve as synchronization maps between structure and noise, by selecting which random pattern in N is added to which structured pattern in P . Indeed, since the masks are synthesized simultaneously with the structure, they can be used to guide the spatial variations of the noise.

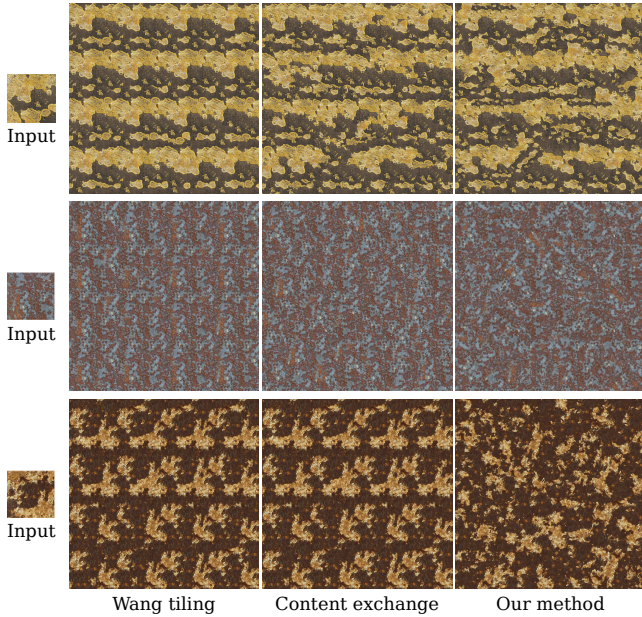


Figure 9: Synthesis results using Wang tiling [CSHD03], content exchange [VSLD13], and content exchange plus rotations and stretching using our bi-layer model.

Let us now discuss the benefits of this bi-layered model over standard, single-layered textures. To synthesize the structure we could use off-line techniques, for example based on graph-cut [KSE*03]. However, we aim at on-the-fly-synthesis. Remember we want to apply deformations. We chose to apply deformations on-the-fly, so as to maximize the variety without extra memory cost. To do so, we modified the mono-scale version of [VSLD13], i.e. without complex color transfers and texture fetches. It consists in Wang tiles, in which patch contents are randomly exchanged. We modified the algorithm by allowing for contents to be rotated (by angle $\theta \in \{\pi/4, \pi/2, 3\pi/4, \pi\}$) and scaled ($0.5 \leq \lambda \leq 1$).

In Figure 9, we compare the results of our technique with related synthesis techniques. Wang tiling exhibits repetitions and alignment artifacts, here, due to a low number of borders (2 times 2 resulting in 16 tiles) and to salient perceptual features on some of the tile borders. The tiles were generated with a patch-based algorithm. Content exchange reduces alignments, but repetitions are still visible. The addition of spatial deformations, made possible by our bi-layer model, reduces repetition artifacts (Figure 9 last column). If applied to a single layer (Figure 10), the fine-scale Gaussian patterns are deformed, strongly altering the appearance. Note also, that our model contributes to hide seams introduced along patch boundaries, in two ways: deformations ease feature alignment along boundaries; the noise layer covers seams and makes them less visible.

In Figure 11, we compare our on-the-fly technique with one of the best current off-line synthesis techniques [KNL*15]. It shows a slight quality loss, which is due to seams in the structure and approximation of the noise spectra. In return, we provide much more

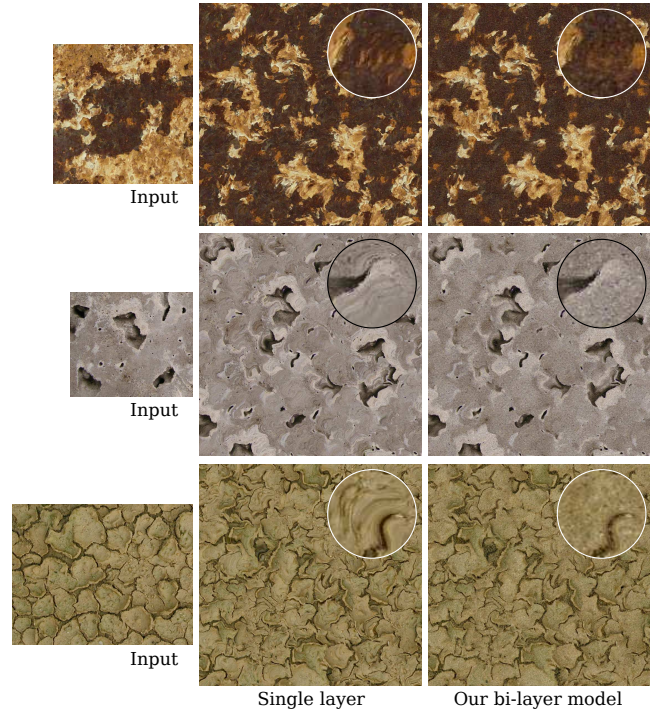


Figure 10: Comparison single layer versus bi-layer. Structure is deformed using scaling, rotations and turbulence. See how the fine patterns are distorted with single layer.

variety, speed (on-the-fly versus tens of minutes) and scalability (unbounded textures).

In Figure 12, we compare with noise by example and LRP-noise [GSV*14] which also separates structure and noise. Our method has several advantages. First, LRP-noise assumes that the noise is stationary while we manage spatial variations, which dramatically increases the set of textures it applies to. Second, our structure has much better quality (see section 5 for details). Third, the structure in [GSV*14] is periodic up to small distortions: rotations or stretching are not possible. Eventually intricate shader implementation is required to reduce the computation overhead due to fixed phases in the structure, while we can rely on any tiling technique.

5. Analysis of input exemplars

In this section, we tackle the problem of instantiating our model from an input exemplar, i.e. computing P , $\{M_k\}$, and $\{S_k\}$ from an input image I . We consider greyscale textures and refer to section 6 for the management of colors.

In Section 3.3 we described a solution to this problem for purely Gaussian, spatially varying noise, i.e. with no structure layer P . We build on this simpler case to solve the full problem (see Figure 4):

- The structure layer P is extracted from I (see details below).
- The noise layer is computed as $N = I - P$.
- The masks M_k are computed as in Section 3.3. Note that the local

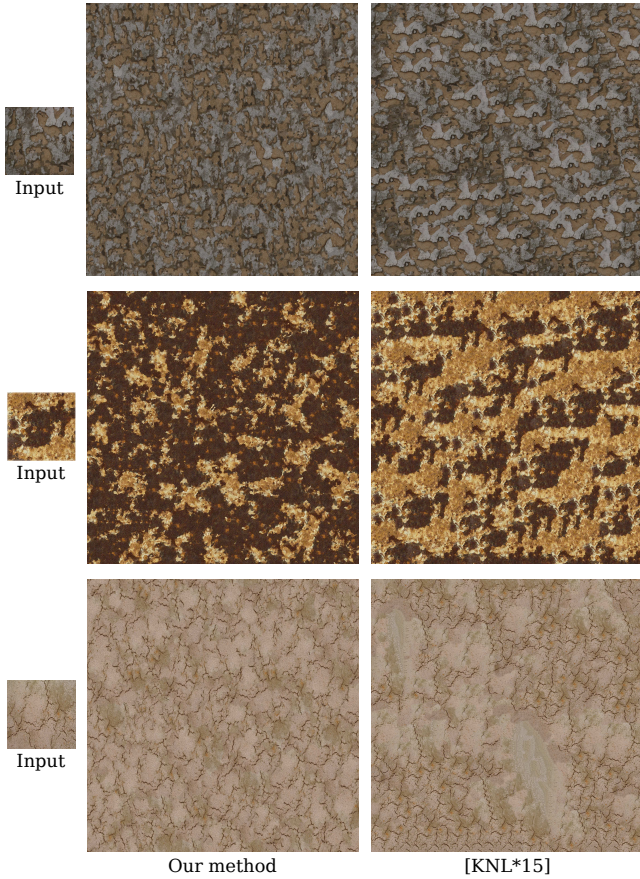


Figure 11: Comparison with off-line optimization [KNL*15]. Optimization reproduces cleaner and sharper features. Our method provides more variety and on-the-fly synthesis.

spectra S_x^{loc} are estimated on I , which contains not only noise. We could have used N instead, however we would have had to do without useful information contained in I , such as the average intensity (or color).

- The global spectra S_k are computed as in Section 3.3. Note that the local spectra are computed on N (not I) because they must encode the noise layer only.

The computation of P from I is somewhat similar to de-texturing and to de-noising, but with important differences preventing us from using some previous solution. We show a comparison in Figure 13 and other ones are provided in the supplemental material. De-texturing [XYXJ12, CLKL14] aims at removing small scale patterns (e.g. tile pieces in a mosaic) while preserving large ones (e.g. the global image of the mosaic). In our case, a criterion for scale is not relevant: in the mosaic example, we would like the piece borders to be kept in P , because they are highly structured. De-noising aims at removing a random additive error from an image, and so do we. Gaussian smoothing adds too much blur. Bilateral filtering performs well, if each region has its own color. However, we want each region to have its own spectrum. Our solution therefore consists in joint bilateral filtering [PKTD09] guided by the lo-

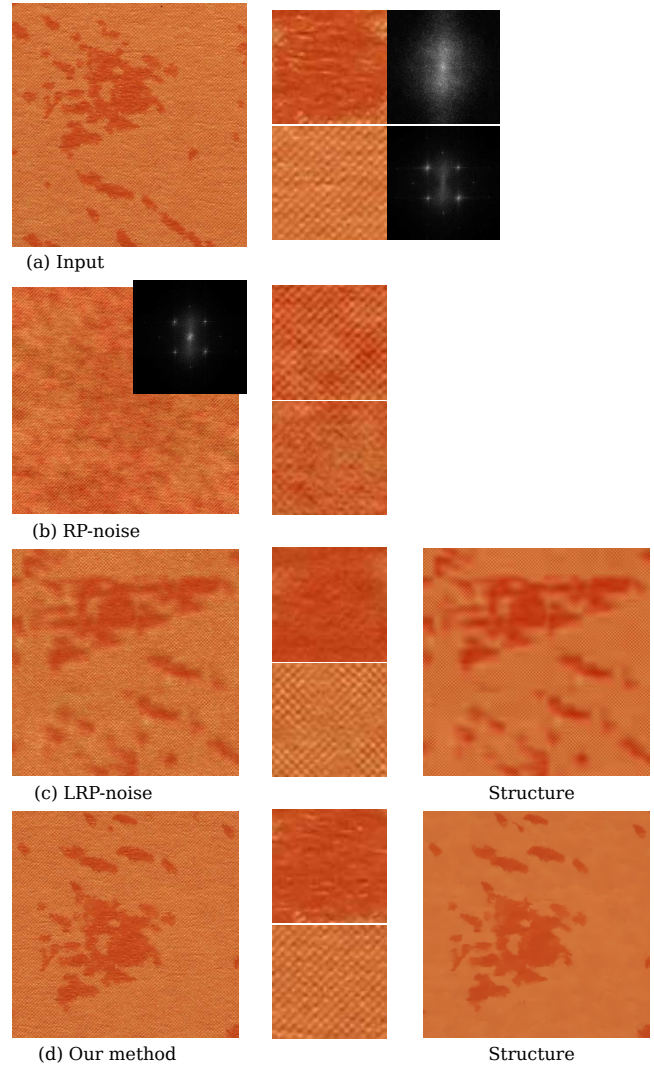


Figure 12: Comparison to noise by example. The example (a) contains two regions with different noises. Random phase noise (b) can not reproduce the underlying structure. Local random phase noise (c) extracts a blurred structure and can not manage spatial variations in the noise. Our technique (d) extracts a sharper structure and well reproduces spatial variations.

cal spectra S_x^{loc} . This way, two pixels x and y are averaged, if they have similar local spectral characteristics. That is, if $\|S_x^{loc} - S_y^{loc}\|$ is small. Our method has proven to be versatile, though de-texturing and bi-lateral filtering also perform well on some examples.

We compared our structure extraction method with [GSV*14], which defines the structure in the spectral domain as the frequencies having the largest magnitude. As noticed by the authors, it mostly selects low frequencies, while high frequencies often contribute to sharp features that we want to be preserved in the structure. Figures 12 and 13 show that our method based on spatial filtering compares favorably.

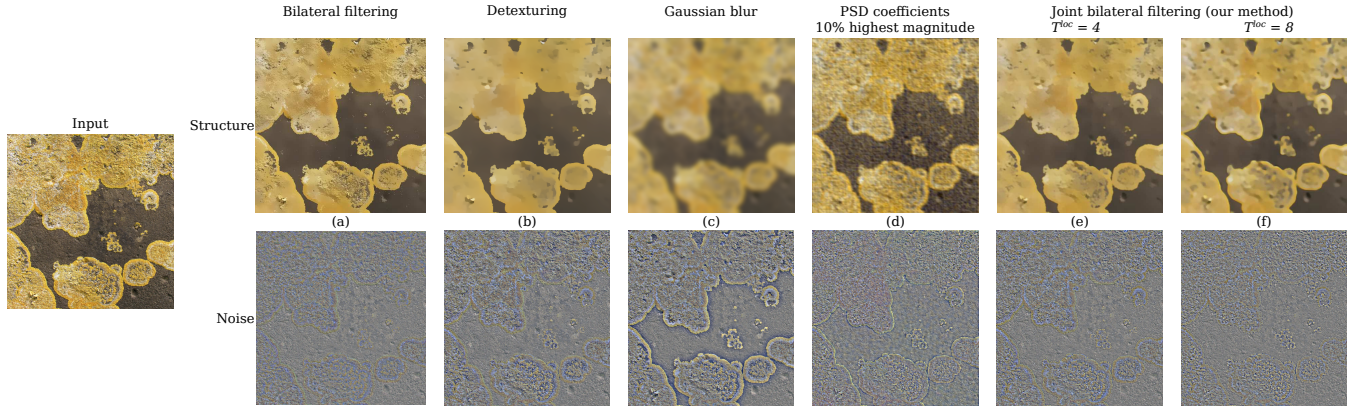


Figure 13: Structure extraction. Bilateral filtering and de-texturing perform well in some cases. Gaussian smoothing blurs sharp edges. Thresholding the PSD fails when high frequencies contribute to the structure. Our joint bilateral filtering driven by local spectra is versatile.

To make the method user-friendly, we only keep a single parameter under the user control. In all our examples, we fixed the joint bilateral filter parameters as follows: spatial neighborhoods are 16 pixels wide; the standard deviation for the distance between spectra is set to 0.01; the filter is iterated 5 times. The only parameter left is the size T^{loc} of the local spectra. The larger T^{loc} , the more information is filtered into N , and possibly the more blurry P will be, leading to possible artifacts in the synthesis. The smaller T^{loc} , the more information is preserved in P , the more faithful the synthesis, but the less deformations can be introduced. We argue that the good value for T^{loc} is the one that produces the best synthesis, which is, in the end, a visual criterion. Thus, we ask the user to select the best size for T^{loc} among a small set of values ($T^{loc} = 2, 4, 8, 16$), based on the visual quality of synthesized examples, see figure 14. The user is shown, for each T^{loc} , the layers P and N , as well as a result with N synthesized over the same P . The best choice is the largest possible T^{loc} leading to acceptable visual results. Many examples are shown in the supplemental material to this paper.

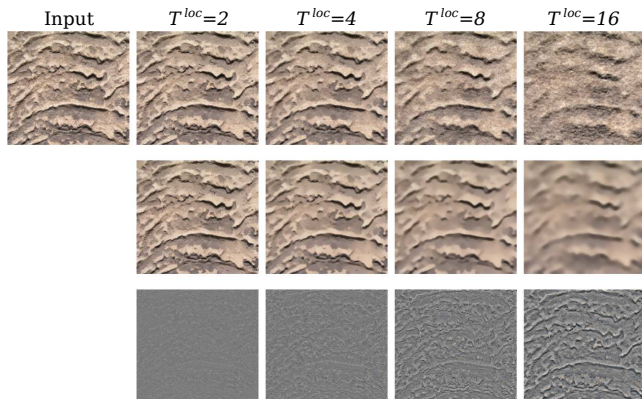


Figure 14: Tuning of the analysis. The user is shown a set of synthesis examples (top) along with the layers P (middle) and N (bottom). He selects the largest value T^{loc} as long as the visual quality is acceptable. Here $T^{loc} = 4$ or 8 would probably be appropriate.

6. Extensions

Colored textures. Colors require modifications in our pipeline. The analysis of a colored input is driven by the luminance channel: local spectra are computed on the luminance, then the computation of masks and the structure extraction are unchanged. This leads to colored layers P and N . The synthesis of structure from P requires no modification. The critical stage is the synthesis of noise because wrong correlations of the RGB channels may create new colors. We treat each noise N_k separately, because they tend to have much less color variations than the global image. Random phase shift [GGM11] can not be used because our PSD estimation provides no phase. So each noise is computed in its own color space with channels as independent as possible, resulting from a per-cluster PCA in the RGB space. The channels are then synthesized independently.

Anti-aliasing. Texture anti-aliasing is an issue when rendering 3D scenes. In particular flickering artifacts are caused by undersampling of large scenes. Our model is compliant with the available techniques for each layer. Regular tilings, which are suitable for the structure layer, generally support MIP-mapping. Note however that no precise pre-filtering is known for content exchange [VSLD13]. The noise layer can be filtered directly in the spectral domain by fading out high frequencies.

Histogram equalization for non-Gaussian noises. Our model a priori requires the noise layer N to be Gaussian, which is not guaranteed. One can loosen this constraint by adding a histogram equalization, that operates on the noise layer only, per-cluster, and per-channel. This widens the set of textures that can be faithfully reproduced, as shown in Figure 15. Moreover, this method is compliant with anti-aliasing [HNPN14].

Improving sharp pattern borders. As discussed in Section 5, choosing the size of local spectra is a compromise: good discrimination of the patterns may require large windows and imply blurring of both the masks and the structure borders. In all our results we used binary masks to sharpen the noise transitions (see Section 3.3). However this does not remove blur in the structure. Fig-

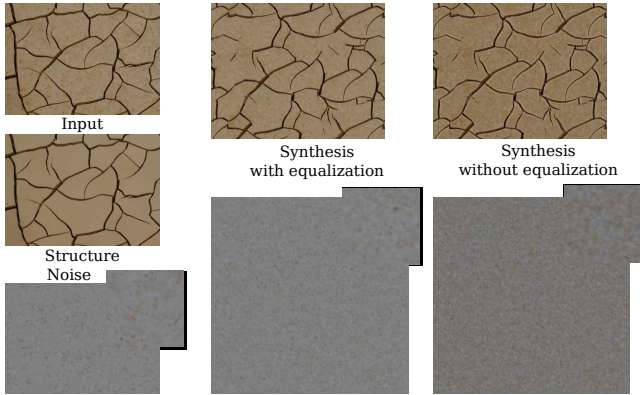


Figure 15: Histogram equalization is applied to the noise layer. It improves synthesis results when the noise is not Gaussian.

ure 16 shows how we can sharpen structure borders by modifying the $P + N$ decomposition. In a small band along the region border N is forced to vanish so sharp borders are preserved in P .

7. Results and discussion

Results. The results of our method are presented through Figures 9 to 16 and in the series of high-resolution images attached as supplementary documents. We showed in Section 3 that we improve over noise-based approaches by controlling spatial variations. We showed in Sections 4 and 5 that our bi-layered model compares favorably to both purely tile-based and LRP-noise approaches. Our method however comes with a number of limitations.

Limitations. Firstly, our method cannot work if fine scale patterns in the input exemplars are not Gaussian. In Figure 17, we show an example where what remains after structure extraction is a structured sub-texture, which cannot be reproduced using a noise model. We could overcome this problem by using our approach in a recursive way, i.e. recursively extracting structure layers until only noise remains. Secondly, several steps of our processing pipeline could be improved. The computation of masks sometimes lack sharpness, and our projection method prevents control of intensity variations because the masks sum up to 1. Also the structure extraction sometimes still blurs borders of some structured patterns (see Figure 16 top).

Performance of the synthesis. The synthesis time is exactly the sum of times for both layers, thus it depends on the algorithms chosen. We implemented the noise layer by large pre-computed periodic tiles: repetition is not visible because of the structure layer. An alternative is to use texton noise [GLM17]. In this context, the bottleneck is the number of texture/memory accesses : 1 for Wang tiles, 2 for patch exchange, $3 + K$ for our technique (when there are less than 4 noises, all masks fit in a single texture). As a comparison, [LH05] requires more than 100 accesses for their full padded pyramid.

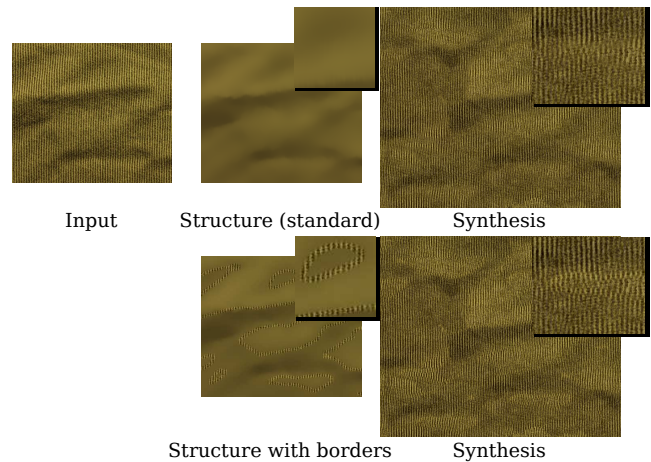
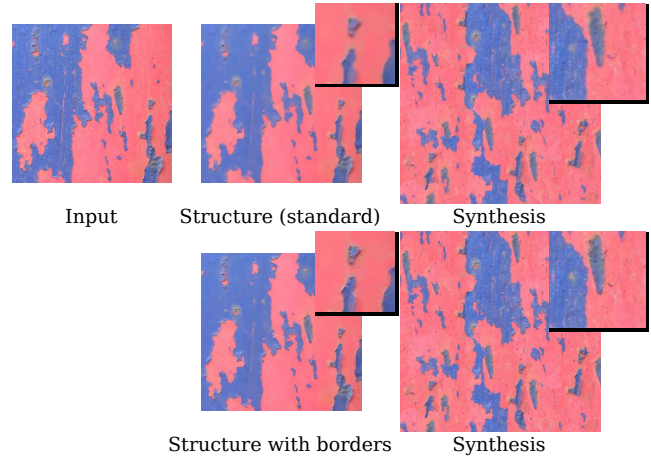


Figure 16: Top row: sharp borders of the input (left) may be smoothed in the structure (middle) and degraded during synthesis (right). Second row: the quality may be improved by exactly preserving a thick border (right) in the structure. In some cases however alignments may be broken (see the fabric).

Performance of the analysis. Many parameters have impact on the off-line analysis, so we provide ranges for 512×512 input exemplars. The main stages of computation are:

- The structure extraction needs a pre-computation of local spectra (1 to 6 min depending on T^{loc}) and the filtering (1 min).
- Computing the masks mainly relies on a K-means clustering, which converges very quickly (less than 20 iterations).
- Estimating the global spectra is the most time consuming, up to 1 hour for 3 channels. It relies on the auto-covariance computation (equation (5)), which depends on the size T , on the sparsity threshold, and on the shape of the masks. Note that this stage is implemented on CPU and could be parallelized.

8. Conclusions

In this paper we presented a new model for spatially varying Gaussian noise, expressed as spatial blending of stationary noises. It

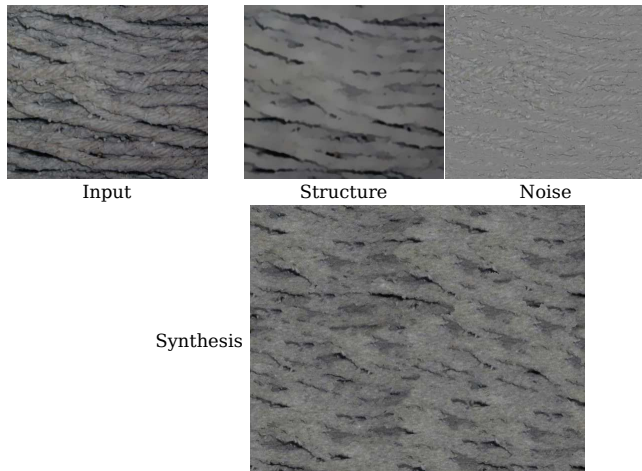


Figure 17: Limitation. The fibers within the noise layer are not Gaussian patterns. Our method fails to synthesize them.

comes with an algorithm for analyzing an input exemplar. Of particular interest is a new spectral estimation technique for noises defined over a region with arbitrary shape (missing data). This model is part of a bi-layered model for representing textures as a sum of a structure layer and a noise layer, synchronized through a set of masks.

Our model supports on-the-fly synthesis, based on random-phase or sparse convolution techniques for the noise layer and tiling for the structure layer. We take advantage of both approaches: tiling well reproduces structured patterns, while noise reduces artifacts. The main advantage of our model is to enable spatial deformations of large structured patterns, while fine Gaussian patterns are preserved. It greatly improves the variety of the synthesized textures.

We provide analysis from an input exemplar. A structure extraction technique is based on joint bilateral filtering. To make this analysis pipeline user-friendly, we carefully reduce user-tuning to two parameters: the number of random patterns (usually 2 to 4); the size of local spectra, for which we provide a visual choice among a few pre-selected values.

Note that while we selected or designed a consistent set of processing methods throughout the pipeline, several of them could be modified or replaced without changing the other stages. In particular, we believe there is room for improvements in the computation of masks and in the extraction of structure, which are closely related to image processing tools.

Another promising perspective is to decide the appropriate deformations from the input itself. While stretching and rotations are easy to tune manually, more complex deformations – such as distortions, bending or shearing – remain challenging.

Besides, some applications are worth being investigated as future extensions of our approach: they include texture transfer, which usually faces distortion problems that could be solved using our bi-layered approach; and texture extraction from images and videos, because it requires pattern description and comparison.

Acknowledgements

This work has been partially funded by the project HDWorlds from the Agence Nationale de la Recherche (ANR-16-CE33-0001) and by the advanced grant 291184 EXPRESSIVE from the European Research Council (ERC-2011-ADG 20110209). We would like to thank Sylvain Thery for the help provided in the development, and Sarah Kushner for english proof-reading. Image Courtesy: www.mayang.com/textures/

References

- [CJMW13] CHEN K., JOHAN H., MUELLER-WITTIG W.: Simple and efficient example-based texture synthesis using tiling and deformation. In *Proceedings of the ACM SIGGRAPH Symposium on Interactive 3D Graphics and Games* (New York, NY, USA, 2013), I3D '13, ACM, pp. 145–152. URL: <http://doi.acm.org/10.1145/2448196.2448219>, doi:10.1145/2448196.2448219. 3
- [CLKL14] CHO H., LEE H., KANG H., LEE S.: Bilateral texture filtering. *ACM Trans. Graph.* 33, 4 (July 2014), 128:1–128:8. URL: <http://cg.postech.ac.kr/research/bt/f/>, doi:10.1145/2601097.2601188. 8
- [CSHD03] COHEN M. F., SHADE J., HILLER S., DEUSSEN O.: Wang tiles for image and texture generation. *ACM Trans. Graph.* 22, 3 (July 2003), 287–294. URL: <http://doi.acm.org/10.1145/882262.882265>, doi:10.1145/882262.882265. 3, 4, 7
- [DG95] DISCHLER J., GHAZANFARPOUR D.: A geometrical based method for highly complex structured textures generation. *Comput. Graph. Forum* 14, 4 (1995), 203–216. URL: <http://dx.doi.org/10.1111/1467-8659.1440203>, doi:10.1111/1467-8659.1440203. 3
- [GDG12] GILET G., DISCHLER J.-M., GHAZANFARPOUR D.: Multiple kernels noise for improved procedural texturing. *Vis. Comput.* 28, 6–8 (June 2012), 679–689. URL: <http://dx.doi.org/10.1007/s00371-012-0711-2>, doi:10.1007/s00371-012-0711-2. 4
- [GGM11] GALERNE B., GOUSSEAU Y., MOREL J.-M.: Random phase textures: Theory and synthesis. *IEEE Transactions on Image Processing* 20, 1 (2011), 257 – 267. 9
- [GLLD12] GALERNE B., LAGAE A., LEFEBVRE S., DRETTAKIS G.: Gabor noise by example. *ACM Trans. Graph.* 31, 4 (July 2012), 73:1–73:9. URL: <http://doi.acm.org/10.1145/2185520.2185569>, doi:10.1145/2185520.2185569. 4, 5
- [GLM17] GALERNE B., LECLAIRE A., MOISAN L.: Texton noise. *Computer Graphics Forum* (2017), n/a–n/a. doi:10.1111/cgf.13073. 4, 5, 10
- [GSV*14] GILET G., SAUVAGE B., VANHOEY K., DISCHLER J.-M., GHAZANFARPOUR D.: Local random-phase noise for procedural texturing. *Transactions on Graphics* 33, 6 (November 2014), 195:1–195:11. (Proceedings of Siggraph Asia'14). doi:10.1145/2661229.2661249. 4, 5, 7, 8
- [HNP14] HEITZ E., NOWROUZSAHRAI D., POULIN P., NEYRET F.: Filtering Non-Linear Transfer Functions on Surfaces. *IEEE Transactions on Visualization and Computer Graphics* 20, 7 (July 2014), 996–1008. URL: <https://hal.inria.fr/hal-00876432>, doi:10.1109/TVCG.2013.102. 9
- [JCW11] JESCHKE S., CLINE D., WONKA P.: Estimating color and texture parameters for vector graphics. *Computer Graphics Forum* 30, 2 (Apr. 2011), 523–532. URL: <https://www.cg.tuwien.ac.at/research/publications/2011/jeschke-2011-est/>. 4
- [KEBK05] KWATRA V., ESSA I., BOBICK A., KWATRA N.: Texture optimization for example-based synthesis. *ACM Trans. Graph.* 24, 3 (July 2005), 795–802. URL: <http://doi.acm.org/10.1145/1073204.1073263>, doi:10.1145/1073204.1073263. 3

- [KNL*15] KASPAR A., NEUBERT B., LISCHINSKI D., PAULY M., KOPF J.: Self tuning texture optimization. *Comput. Graph. Forum* 34, 2 (2015), 349–359. URL: <http://dx.doi.org/10.1111/cgfm.12565>, doi:10.1111/cgfm.12565. 2, 7, 8
- [KSE*03] KWATRA V., SCHÖDL A., ESSA I., TURK G., BOBICK A.: Graphcut textures: Image and video synthesis using graph cuts. In *ACM SIGGRAPH 2003 Papers* (New York, NY, USA, 2003), SIGGRAPH '03, ACM Siggraph, ACM, pp. 277–286. URL: <http://doi.acm.org/10.1145/1201775.882264>, doi:10.1145/1201775.882264. 4, 7
- [LD06] LAGAE A., DUTRÉ P.: An alternative for wang tiles: Colored edges versus colored corners. *ACM Trans. Graph.* 25, 4 (Oct. 2006), 1442–1459. URL: <http://doi.acm.org/10.1145/1183287.1183296>, doi:10.1145/1183287.1183296. 3, 4
- [LH05] LEFEBVRE S., HOPPE H.: Parallel controllable texture synthesis. *ACM Trans. Graph.* 24, 3 (July 2005), 777–786. URL: <http://doi.acm.org/10.1145/1073204.1073261>, doi:10.1145/1073204.1073261. 3, 10
- [LL12] LASRAM A., LEFEBVRE S.: Parallel patch-based texture synthesis. In *Proceedings of the Fourth ACM SIGGRAPH / Eurographics Conference on High-Performance Graphics* (Aire-la-Ville, Switzerland, Switzerland, 2012), EGGH-HPG'12, Eurographics Association, pp. 115–124. URL: <http://dx.doi.org/10.2312/EGGH/HPG12/115-124>, doi:10.2312/EGGH/HPG12/115-124. 3
- [LLC*10] LAGAE A., LEFEBVRE S., COOK R., DEROSE T., DRETAKIS G., EBERT D., LEWIS J., PERLIN K., ZWICKER M.: A survey of procedural noise functions. *Computer Graphics Forum* 29, 8 (2010), 2579–2600. URL: <http://dx.doi.org/10.1111/j.1467-8659.2010.01827.x>, doi:10.1111/j.1467-8659.2010.01827.x. 3
- [LLH04] LIU Y., LIN W.-C., HAYS J.: Near-regular texture analysis and manipulation. In *ACM SIGGRAPH 2004 Papers* (New York, NY, USA, 2004), SIGGRAPH '04, ACM, pp. 368–376. URL: <http://doi.acm.org/10.1145/1186562.1015731>, doi:10.1145/1186562.1015731. 3
- [LSA*16] LOCKERMAN Y. D., SAUVAGE B., ALLÈGRE R., DISCHLER J.-M., DORSEY J., RUSHMEIER H.: Multi-scale label-map extraction for texture synthesis. *ACM Trans. Graph.* 35, 4 (July 2016), 140:1–140:12. URL: <http://doi.acm.org/10.1145/2897824.2925964>, doi:10.1145/2897824.2925964. 4
- [PKTD09] PARIS S., KORNPBST P., TUMBLIN J., DURAND F.: Bilateral filtering: Theory and applications. *Foundations and Trends® in Computer Graphics and Vision* 4, 1 (2009), 1–73. URL: <http://dx.doi.org/10.1561/06000000020>, doi:10.1561/06000000020. 8
- [RCOL09] ROSENBERGER A., COHEN-OR D., LISCHINSKI D.: Layered shape synthesis: Automatic generation of control maps for non-stationary textures. In *ACM SIGGRAPH Asia 2009 Papers* (New York, NY, USA, 2009), SIGGRAPH Asia '09, ACM, pp. 107:1–107:9. URL: <http://doi.acm.org/10.1145/1661412.1618453>, doi:10.1145/1661412.1618453. 4
- [Sta97] STAM J.: *Aperiodic texture mapping*. Tech. Rep. ERCIM-01/97-R046, European Research Consortium for Informatics and Mathematics (ECRIM), 1997. 3
- [VSLD13] VANHOEY K., SAUVAGE B., LARUE F., DISCHLER J.-M.: On-the-fly multi-scale infinite texturing from example. *ACM Trans. Graph.* 32, 6 (Nov. 2013), 208:1–208:10. URL: <http://doi.acm.org/10.1145/2508363.2508383>, doi:10.1145/2508363.2508383. 3, 4, 7, 9
- [vW91] VAN WIJK J. J.: Spot noise texture synthesis for data visualization. *SIGGRAPH Comput. Graph.* 25, 4 (July 1991), 309–318. URL: <http://doi.acm.org/10.1145/127719.122751>, doi:10.1145/127719.122751. 4
- [Wel67] WELCH P. D.: The use of fast fourier transform for the estimation of power spectra: A method based on time averaging over short, modified periodograms. *IEEE Transactions on Audio and Electroacoustics* 15, 2 (Jun 1967), 70–73. doi:10.1109/TAU.1967.1161901. 5
- [WLKT09] WEI L.-Y., LEFEBVRE S., KWATRA V., TURK G.: State of the art in example-based texture synthesis. In *Eurographics 2009, State of the Art Report, EG-STAR* (2009), Eurographics Association. URL: <http://www-sop.inria.fr/revs/Basilic/2009/WLKT09.3>
- [WWY14] WU R., WANG W., YU Y.: Optimized synthesis of art patterns and layered textures. *IEEE Transactions on Visualization and Computer Graphics* 20, 3 (March 2014), 436–446. doi:10.1109/TVCG.2013.113. 4
- [WY04] WU Q., YU Y.: Feature matching and deformation for texture synthesis. *ACM Trans. Graph.* 23, 3 (Aug. 2004), 364–367. URL: <http://doi.acm.org/10.1145/1015706.1015730>, doi:10.1145/1015706.1015730. 4
- [XFPA14] XIA G.-S., FERRADANS S., PEYRÉ G., AUJOL J.-F.: Synthesizing and mixing stationary gaussian texture models. *SIAM Journal on Imaging Sciences* 7, 1 (2014), 476–508. URL: <https://hal.archives-ouvertes.fr/hal-00816342>, doi:10.1137/130918010. 5
- [XYXJ12] XU L., YAN Q., XIA Y., JIA J.: Structure extraction from texture via relative total variation. *ACM Trans. Graph.* 31, 6 (Nov. 2012), 139:1–139:10. URL: <http://www.cse.cuhk.edu.hk/leojia/projects/texturesep/index.html>, doi:10.1145/2366145.2366158. 8
- [ZFCVG05] ZALESNY A., FERRARI V., CAENEN G., VAN GOOL L.: Composite texture synthesis. *Int. J. Comput. Vision* 62, 1-2 (Apr. 2005), 161–176. URL: <http://dx.doi.org/10.1007/s11263-005-4640-7>, doi:10.1007/s11263-005-4640-7. 4